

Aggregate Frequency Width, Nuclear Hyperfine Coupling and Jahn-Teller Effect of Cu^{2+} Impurity Ion ESR in $SrLaAlO_4$ Dielectric Resonator at 20 Millikelvin

M. A. Hosain,^{1, a)} J.-M. Le Floch,^{2, 1} J. Krupka,³ and M. E. Tobar¹

¹ARC Centre of Excellence for Engineered Quantum Systems, School of Physics, University of Western Australia, 35 Stirling Highway, Crawley WA 6009, Australia.

²MOE Key Laboratory of Fundamental Physical Quantities Measurement, School of Physics, Huazhong University of Science and Technology, Wuhan 430074, Hubei, China.

³Department of Electronics and Information Technology, Institute of Microelectronics and Optoelectronics, Warsaw University of Technology, Koszykowa 75, 00-662 Warszawa, Poland.

The impurity paramagnetic ion, Cu^{2+} substitutes Al in the $SrLaAlO_4$ single crystal lattice, this results in a CuO_6 elongated octahedron, the resulting measured g-factors shows four-fold axes variation condition. The aggregate frequency width of the electron spin resonance with the required minimum level of impurity concentration has been evaluated in single crystal $SrLaAlO_4$ at 20 millikelvin. Measured parallel hyperfine constants, $A_{\parallel Cu}$, were determined to be $-155.7 \times 10^{-4} \text{ cm}^{-1}$, $-163.0 \times 10^{-4} \text{ cm}^{-1}$, $-178.3 \times 10^{-4} \text{ cm}^{-1}$ and $-211.1 \times 10^{-4} \text{ cm}^{-1}$ at 9.072 GHz ($WGH_{4,1,1}$) for the nuclear magnetic quantum number $M_I = +\frac{3}{2}, +\frac{1}{2}, -\frac{1}{2}$, and $-\frac{3}{2}$ respectively. The anisotropy of the hyperfine structure reveals a characteristics of static Jahn-Teller effect. The second-order-anisotropy-term, $\sim (\frac{\text{spin-orbit coupling}}{10D_q})^2$, is significant and can not be disregarded, with the local strain dominating over the observed Zeeman-anisotropy-energy difference. The Bohr electron magneton, $\beta = 9.23 \times 10^{-24} \text{ JT}^{-1}$, (within -0.43% so-called experimental error) has been found using the measured spin-Hamiltonian parameters. Measured nuclear dipolar hyperfine structure parameter $P_{\parallel} = 12.3 \times 10^{-4} \text{ cm}^{-1}$ shows that the mean inverse third power of the electron distance from the nucleus is $\langle r_q^{-3} \rangle \simeq 5.23$ a.u. for Cu^{2+} ion in the substituted Al^{3+} ion site assuming nuclear electric quadruple moment $Q = -0.211$ barn.

A. Introduction:

Recently there has been renewed interests and experimental studies devoted to spins in solids due to the emergence of new quantum hybrid systems, which requires the manipulation of spin quantum states¹⁻³, with continued searches for viable candidates^{2,4}. In this work, we implement the whispering gallery (WG) mode technique to study impurity paramagnetic ions unpaired electron spin resonance possessing nuclear hyperfine coupling in a dielectric crystal lattice⁵⁻⁷. Site symmetry information of impurity paramagnetic ions in the $SrLaAlO_4$ (SLA) single crystal lattice is acquired through WG multi mode ESR spectroscopy (Fig.1,2,3 and 4), providing measurement of hyperfine structure broadening, g-factor variation and other anisotropy effects.

WG mode spectroscopy is highly sensitive, combined with the multi-mode nature of the experimental results provides values of some fundamental physics quantities with high precision. The Jahn-Teller effect in a metal-ligand octahedral complex, ML_6 , usually induces charge coupling, orbital and magnetic ordering, displacement, and underlines the structural details in determining electronic behaviour⁸⁻¹¹. Such kind of high precision measurements of the hyperfine structure characteristics are essential for quantum state mapping. The unpaired electron spin moment reveals information about the spin-

Hamiltonian parameters, including hyperfine structure anisotropy in a single spectroscopic term of anomalous Zeeman transitions when each WG mode of resonance frequency, ω , is equal to the Larmor precession, ω_L , of the magnetic dipoles^{5,6,12}. Also, it is possible to determine the difference in the spin-Hamiltonian parameters due to tetragonal distortions using ESR spectroscopy^{13,14}. Luminescence and phosphorescence were determined in other perovskite crystals with Cu^{2+} defect centres as well^{15,16}. Feng and Zheng¹⁷ gave a theoretical analysis of spin-Hamiltonian parameters for the rhombic Cu^{2+} centres in $CuGaSe_2$ crystal. A suitable low-loss crystal is required for possible use as a host of paramagnetic ions for this ESR study. Sequential excitation of WG modes of X-band to Ku-band frequencies in the low-loss $SrLaAlO_4$ dielectric bulk crystal under systematic control of high resolution vector network analyzer (VNA) with a sophisticated coupled co-axial loop allows us to perform these measurements and analysis. In this dielectric resonance process, the WG modes energy loss mechanisms was minimized achieving a high loaded Q-factor Q_L for this ESR spectroscopy at 20 millikelvin (mK)¹⁸⁻²¹.

High confinement of electromagnetic field in the low-loss crystal $SrLaAlO_4$ (SLA) ensures high sensitivity of ESR spectroscopy for very low concentration of impurity ions. Implementing this technique, the microwave-power and other terms are kept constant, the required minimum number of impurity ion follows the proportionality^{22,23} $N_{min} \propto \frac{1}{\omega Q_L}$ for detection of ESR transition spectrum, and is estimated for Cu^{2+} ion of unpaired electron effec-

^{a)}Electronic mail: akhter361@yahoo.co.uk

tive spin $S = \frac{1}{2}$ as:

$$N_{min} = \left(\frac{4k_B V_s T_s}{g_e^2 \beta^2 \mu_o} \right) \left(\frac{\Delta\omega}{\omega} \right) \left(\frac{1}{\eta Q_L} \right) \left(\frac{P_n}{P} \right)^{\frac{1}{2}} \quad (1)$$

Where k_B is the Boltzman constant, V_s is the mode volume, T_s is the sample temperature, g_e is the electron g-factor, β is the Bohr electron magneton, μ_o is the magnetic permeability of free space, ω is the resonance frequency (or transition energy frequency), η is the filling factor, P_n is the noise intensity, P is the microwave input intensity, and $\Delta\omega$ is the width of aggregated spin frequency at resonance which is depended on the 'shape function' $f(\omega)$ normalized as $\int_0^\infty f(\omega) \partial\omega = 1$ for a wide range of Larmor precession. Significant output (transmission) occurs only at the resonance in a very narrow frequency width $\Delta\omega$ in the region $\omega \approx \omega_L$ for ESR (Fig. 1). Previously, many studies devoted to high sensitive measurements of various types of resonators over a wide range of frequencies with a variety of probing system have been performed²⁴⁻²⁸. Benmessai et al.⁶ described a typical concentration level measurement of impurity Fe^{3+} ion in sapphire using WG mode microwave resonance. Anders et al.²⁷ described a single-chip electron spin resonance detector operating at 27 GHz.

The single crystal $SrLaAlO_4$ crystallizes in a K_2NiF_4 -structure of space group $I4/mmm$ with the lattice constants of $a = b = 3.756 \text{ \AA}$ and $c = 12.636 \text{ \AA}$, grown by the Czochralski technique²⁹⁻³². The Al^{3+} site is surrounded by a tetragonally elongated (along c-axis) oxygen octahedron of two bonds $Al - O2$ of length $R_{||} = 2.121 \text{ \AA}$ and four coplanar bonds $Al - O1$ of length $R_{\perp} = 1.885 \text{ \AA}$ between aluminium and oxygen^{32,33}. In the substituted Al^{3+} ion site, the d^9 ground state of Cu^{2+} ion $|x^2 - y^2\rangle = |2^s\rangle$ orbital singlet of spin doublet (super-script 's' indicates symmetric wave function) is valid to consider as a cubic symmetry with small deformation in the CuO_6 octahedral structure of complex due to elongation along z-axis (c-axis) under tetragonal distortion^{34,35}. Hence, an applicable hyperfine spin-Hamiltonian in the z-axis symmetry of ion of nuclear spin I with electron effective spin $S = \frac{1}{2}$ takes the form³⁵:

$$\mathcal{H}_n = A_{||Cu} S_z I_z + A_{\perp Cu} (S_x I_x + S_y I_y) + P_{||} \left\{ I_z^2 - \frac{1}{3} I(I+1) \right\} - \beta B g_{||Cu}^I I_z \quad (2)$$

$A_{||Cu}$ and $A_{\perp Cu}$ are parallel and perpendicular component of hyperfine constant \mathbf{A} , the magnetic field is \mathbf{B} applied along z-axis and $g_{||Cu}^I$ is the nuclear parallel g-factor aligned with electronic parallel g-factor $g_{||Cu}$. The dipolar hyperfine structure parameter is considered due to interaction with electric quadrupole moment of nucleus Q , which is in this symmetry $P_{||} = -\frac{3e^2 Q}{7I(2I-1)} \langle r_q^{-3} \rangle$. Where $\langle r_q^{-3} \rangle$ is the mean inverse third power of the electron distance from the nucleus (origin), averaged

over the electronic wave-functions. For the unfilled d-shell paramagnetic unpaired electron, this term is $\langle r^{-3} \rangle = \frac{\langle r_q^{-3} \rangle}{1-R_q}$, where R_q is 0.1 to 0.2 approximately.

The hyperfine structure lines are separated by an amount of magnetic field $\frac{A}{g_e \beta}$ (considering 1st order perturbation)³⁴. Along the crystal symmetry axis z, the hyperfine structure anisotropy (Fig. 2, 3 and 4) plays the roles with anisotropy energy^{34,35}:

$$W = P_{||} \left\{ I_z^2 - \frac{1}{3} I(I+1) \right\} - \beta B g_{||Cu}^I I_z \quad (3)$$

The condition $\beta B g_{||Cu} \gg A_{||Cu} \gg P_{||} \gg \beta B g_{||Cu}^I$ is implied for the hyperfine multiplet observations from a single spectroscopic term. Nuclear Zeeman energy term $\beta B g_{||Cu}^I$ is naturally very small, and Bleaney et al^{36,37} measured $P_{||}$ of Cu^{2+} ion is about 0.0011 cm^{-1} in both tutton salts and lanthanum magnesium nitrate at 20 K. We keep temperature $T \leq 20 \text{ mK}$ steadily maintaining a possible state of $k_B T < A_{||Cu}$ for observation and measurement of hyperfine structure including anisotropies as nuclear dipolar hyperfine interaction.

B. Aggregate frequency width of WG mode ESR spectrum and impurity ion concentration:

A light-yellow cylindrical $SrLaAlO_4$ crystal of height 9.04 mm and diameter 17.18 mm was inserted at the center of an oxygen-free cylindrical copper cavity. The crystal loaded cavity was cooled in a dilution refrigerator (DR) down to 20 mK, with the low temperature improving the sensitivity as shown in Eq.1. Fifteen WG modes with high-azimuthal-mode-number within a frequency range of 7 GHz to 18 GHz, and thus electromagnetic energy filling factors of the order of unity were monitored. The applied DC-magnetic field is auto-controlled through the electric current to the superconducting magnet by computer program. The magnetic field within the range -0.2 T to 1 T was applied ensuring by the computer in a step of sweep $4 \times 10^{-4} \text{ T}$ maintaining stabilized temperature at 20 mK. Each mode with frequency span 2 MHz was scanned in a very narrow frequency line width of a high resolution VNA for a period of five seconds at each step of magnetic field. The slow rate of sweep of magnetic field was applied keeping stabilized temperature. The microwave input power of the SLA resonator was about -60 dBm . Mode volume of the order 10^{-7} m^3 , and Q_L about 100,000 at 20 mK. Aggregate frequency width $\Delta\omega \leq 50 \text{ kHz}$ is in the region $\omega \approx \omega_L$ for hybrid mode $WGH_{4,1,2}$ of resonance frequency 9.121 GHz and Q_L about 75,000 (Fig.1). Also, the $WGH_{4,1,1}$ had³⁸ $\Delta\omega \leq 20 \text{ kHz}$ in the region $\omega \approx \omega_L$ of resonance frequency 9.072 GHz and Q_L about 115,000. With a little dielectric variation among selected modes, observed Q_L was always more than 50,000 at 20 mK.

In such a observed viable state, practically $\Delta\omega$ was less than line-width of all the selected WG modes. Hence the minimum number of ion (effective spin $S = \frac{1}{2}$) is required about 3×10^{10} within the WG mode volume at a noise level of ratio $\frac{P_n}{P} = 1$ (see Eq.1). These adjustments ensure the sensitivity of this method at 20 mK in *SrLaAlO₄* crystal of *Cu²⁺* ion allowing detection down to the 0.03 ppb level of concentration.

For this technique, the factor $\frac{\Delta\omega}{\omega}$ in Eq.1 determines the required measurement accuracy²³ under influence of hyperfine coupling and effective spin S. Because, we can observe $\Delta\omega$ from the transmission spectrum density plot (Fig.1) and adjust the required Q-factor according to $\Delta\omega$. The number N_{min} changes as a product with the term $\frac{3}{S(S+1)}$. On the other hand, in case of the calculation of N_{min} as a notion of $\frac{spins}{G}$, the factor $\frac{\Delta B}{B}$ is used²³ instead of $\frac{\Delta\omega}{\omega}$ in the Eq.1. Here ΔB is the line width, B is the resonant magnetic field and $1G = 10^{-4}T$.

To avoid the addition of thermal noise from room temperature, a 10 dB microwave attenuator was used at 4 K stage and another one at 1 K stage of the DR. Also, a 20 dB attenuator was added at 20 mK stage of the DR. These cold stage attenuation plus the use of a low noise temperature cryogenic amplifier at the output after the resonator ensures good enough signal to noise ratio (SNR). From these ESR characteristics, we were able to identify the types of paramagnetic impurities present in the crystal with hyperfine couplings.

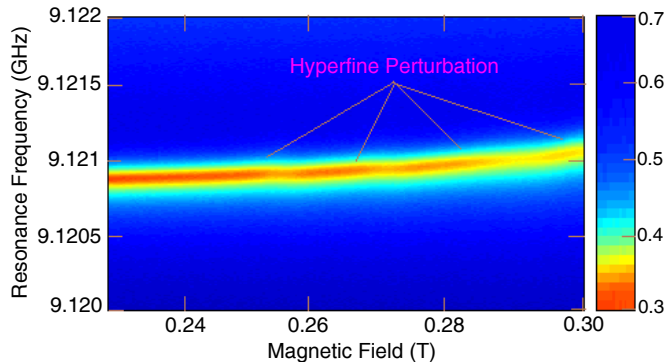


FIG. 1. Density plot of *Cu²⁺* ion ESR spectrum showing aggregate frequency width (width of deep red background) about 50kHz of aggregate spin ensemble around resonance frequency 9.121GHz of *WGH_{4,1,2}* mode. Background frequency shift with the increase of magnetic field is due to local strain.

C. Results and Discussion:

1. Hyperfine structure anisotropy:

The measured hyperfine multiplet of different resonance frequencies in a structure of four lines in the

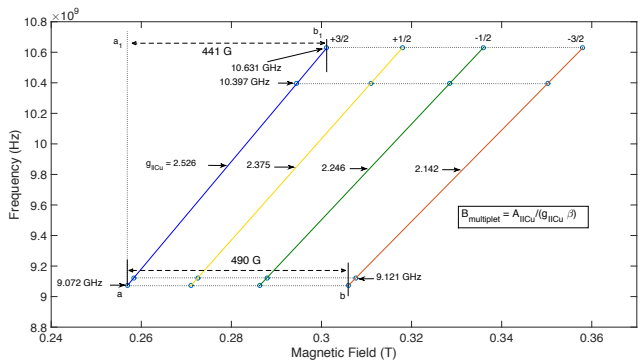


FIG. 2. g-factor and hyperfine structure anisotropy map of *Cu²⁺* ion with *WG* modes of different frequency of ESR spectrum. The magnetic field under hyperfine coupling is $\mathbf{B} = \mathbf{B}_0 - \frac{\mathbf{A}M_I}{g_e\beta}$; and resonance frequency $\omega = -\gamma\mathbf{B}_0$. The magnetic field \mathbf{B}_0 is the external magnetic field of resonance without hyperfine coupling, and γ is the gyromagnetic ratio of electron.

ESR spectrum map (Fig. 2) indicates an ion of $I = \frac{3}{2}$ which is the nuclear spin of *Cu²⁺* ion. It reveals hyperfine multiplets with a substantial anisotropy. The hyperfine structure width varies by 79 G from 132 G to 211 G as nuclear magnetic quantum number, M_I , varies from $+\frac{3}{2}$ to $-\frac{3}{2}$; and the broadening increases with the increase of applied magnetic field (Fig. 2 and 3). As a consequence, the measured parallel g-factors $g_{\parallel Cu}$ are of 2.526, 2.375, 2.246 and 2.142 (Fig. 2). The amount of hyperfine multiplet magnetic field in the Fig.2 are given as the hyperfine structure anisotropy of the four identified WG modes of resonance frequencies 9.072 GHz, 9.121 GHz, 10.397 GHz and 10.631 GHz. For each *WG* mode, it is showing $A_{\parallel Cu}$ variation between nuclear spin quantum numbers $+\frac{3}{2}$ to $-\frac{3}{2}$ (Fig. 2). These broadening effects are happening with the reduction of parallel g-factor between the steps of nuclear magnetic quantum numbers. In this perturbation, magnetic field varies according to M_I , and multiplet width may be written as³⁴ $\frac{A_{\parallel Cu}}{g_{\parallel Cu}\beta}$ (Fig.2 and 3). The observed variation of multiplet's magnetic field width among M_I , of $+\frac{3}{2}$ to $-\frac{3}{2}$ is apparently due to nuclear electric quadruple moment producing impact as dipolar hyperfine structure parameter (P_{\parallel}). These observations of spectroscopic terms are in a good agreement with theoretical models.

Basically, the formulas of spin-Hamiltonian parameters are considered with a typical value of $\frac{\lambda}{\Delta} \sim -0.05$ in the crystal field³⁵. Here, λ is the spin-orbit coupling constant and $\Delta = 10D_q$ is the energy difference between t_{2g} and e_g . But the correction term $\sim (\frac{\lambda}{\Delta})^2$ is not negligible for the most general case of a rhombic distortions^{35,36,39}, which admixes the e_g splitted doublet (splitting due to the tetragonal distortion) ground state $|x^2 - y^2\rangle = |2^s\rangle$ with $|3z^2 - r^2\rangle = |0\rangle$. For the ground state $|2^s\rangle$ in

TABLE I. Spin-Hamiltonian parameters of Cu^{2+} ion in $SrLaAlO_4$, and mean values for the two stable isotopes ^{63}Cu , ^{65}Cu in $[La_2Mg_3(NO_3)_{12}, (24H_2O \text{ or } 24D_2O)]$: Hyperfine structure constants \mathbf{A} and \mathbf{P} are in units of 10^{-4} cm^{-1} .

Source	Temperature	g -factors	\mathbf{A} and \mathbf{P}
Theoretical ³³ ($SrLaAlO_4$)		$g_{\parallel Cu} = 2.321$ $g_{\perp Cu} = 2.070$	$A_{\parallel Cu} = -150$ $A_{\perp Cu} = -3$
Experimental ⁴¹ ($SrLaAl_{1-x}Cu_xO_4$) $x = 0.02$	293 K	$g_{\parallel Cu} = 2.321$ $g_{\perp Cu} = 2.069$	$A_{\parallel Cu} = -150$ $A_{\perp Cu} < 10$
This Experiment ($SrLaAlO_4$)	20 mK	$g_{\parallel Cu} = 2.322$ $g_{\perp Cu} = 2.053$ $\frac{1}{3}(g_{\parallel Cu} + 2g_{\perp Cu})$ $= 2.142(6)$	$A_{\parallel Cu} = -174.6$ $A_{\perp Cu} = 13.4$ $\frac{1}{3}(A_{\parallel Cu} + 2A_{\perp Cu})$ $= -49.26$ $P_{\parallel} = +12.3$
Experimental ^{36,37} $[La_2Mg_3(NO_3)_{12}]$	90 K	$g_{\parallel Cu} = 2.219(3)$ $g_{\perp Cu} = 2.218(3)$	$ A_{\parallel Cu} = 29.0(5)$ $ A_{\perp Cu} = 27.5(5)$
Experimental ^{9,37} $[La_2Mg_3(NO_3)_{12}]$	20 K	$g_{\parallel Cu} = 2.465(1)$ $g_{\perp Cu} = 2.099(1)$ $\frac{1}{3}(g_{\parallel Cu} + 2g_{\perp Cu})$ $= 2.221(1)$	$A_{\parallel Cu} = -111.7(5)$ $ A_{\perp Cu} = 16.0(5)$ $\frac{1}{3}(A_{\parallel Cu} + 2A_{\perp Cu})$ $= 26.6(5)$ $P_{\parallel} = +10.5(5)$

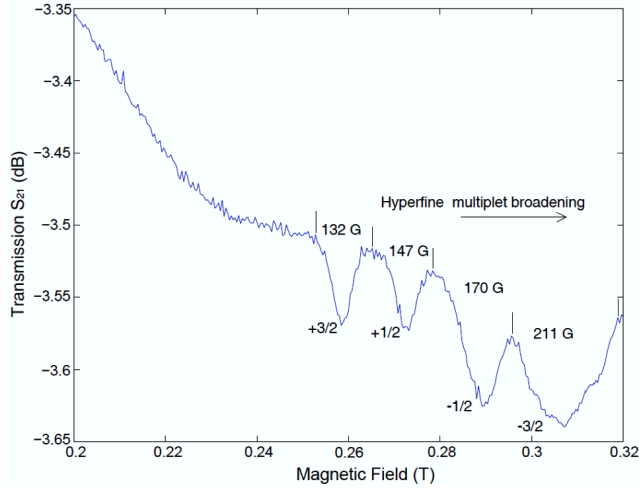


FIG. 3. Hyperfine multiplet widths of Cu^{2+} ion nuclear perturbation coupling with $WGH_{4,1,1}$ mode of frequency 9.072 GHz at 20 mK .

octahedral elongation along z -axis due to the tetragonal distortion, the parallel and perpendicular g -factors anisotropy are $\delta(g_{\parallel Cu}) = 8 \times \frac{\Delta}{\Lambda}$ and $\delta(g_{\perp Cu}) = 2 \times \frac{\Delta}{\Lambda}$ respectively (considering crystal field splitting between e_g and t_{2g} in average equal to Δ)^{36,40}.

Taking average of the measured parallel g -factors, the parallel g -factor anisotropy $\delta(g_{\parallel Cu})$ is about 0.32. Using the values of measured $g_{\parallel Cu}$, calculated perpendicular g -factor anisotropies are $\delta(g_{\perp Cu}) \simeq 0.051$ in $SrLaAlO_4$ crystal. From the formula, taking $\Delta \sim 12,300 \text{ cm}^{-1}$, these g -factor anisotropy values ~ 0.4 of parallel g -factor and ~ 0.1 of perpendicular g -factor were measured by Bleaney et al.^{36,37}. They considered Cu^{2+} ion in a crystal like lanthanum magnesium nitrate salt where Cu^{2+} is at the site of substituted diamagnetic Mg^{2+} ion (see Table-I). The measured values of g -factor

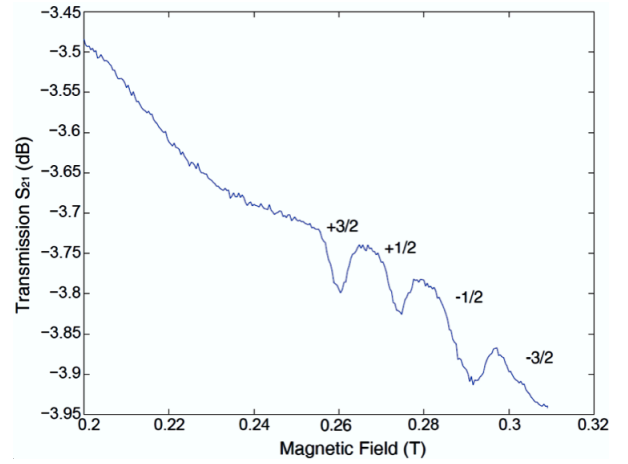


FIG. 4. Hyperfine multiplet widths of Cu^{2+} ion nuclear perturbation coupling with $WGH_{4,1,2}$ mode of frequency 9.121 GHz at 20 mK . Transmission spectrum disappeared at the position of $M_I = -\frac{3}{2}$ (magnetic field 0.31 T) due to local strain in the CuO_6 octahedral structure.

anisotropy in $SrLaAlO_4$ are slightly smaller than their measured values of g -factor anisotropy, plausibly the cause of co-valency effect in the divalent Cu^{2+} ion site of the substituted trivalent Al^{3+} ion. It may be mentioned that Al^{3+} ion is not diamagnetic, and its outermost electron shell is p -orbital which is quenched in ESR transitions. Also, the measured values agreed with the theoretical condition $g_{\parallel Cu} > g_{\perp Cu} > g_s$, which is implied for the elongation along z -axis (g_s is the free electron g -factor).

In the O^{2-} ions coplanar bonds in four fold axis (of four $Cu - O1$ bonds and two elongated $Cu - O2$ bonds), a hole de-localization due to metal-ligand charge transfer is considered⁴¹. Divalent copper oxidation stage $+2.46$ in the substituted trivalent Al^{3+} ion site supports this arguments as a consequence of partial hole contribution⁴¹. Iodometric titration gives this average value of the copper oxidation (of $+2.46$) for the formatted hole in CuO_6 center of $Al_{1-x}Cu_xO_2$ with $x = 0.2, 0.4, 0.6$ and 0.8 solid solution⁴². Yu. V. Yablokov et al.⁴¹ observed that the lattice constant, c , is strongly influenced by the copper concentration. They found that in $LaSrAl_{1-x}Cu_xO_4$, for $x = 1$ the value $c = 12.97 \text{ \AA}$ virtually coincides with the value 13.11 \AA .

Hence, naturally the substitution of divalent Cu^{2+} ion in trivalent Al^{3+} ion site changes the stoichiometry and has significant effect on ESR spectrum, but the influence of concentration has been disregarded for such a low concentration level (of the order of ppb) of impurity Cu^{2+} ion in case of the crystal $SrLaAlO_4$. Since the ionic radius of copper ($r_{Cu} = 0.72 \text{ \AA}$) is larger than the substituted aluminium ion radius ($r_{Al} = 0.51 \text{ \AA}$), Wei et al.³³ found that this causes a displacement making the $Cu - O1$ bond length $R'_{\perp} = 1.945 \text{ \AA}$ shifting away the

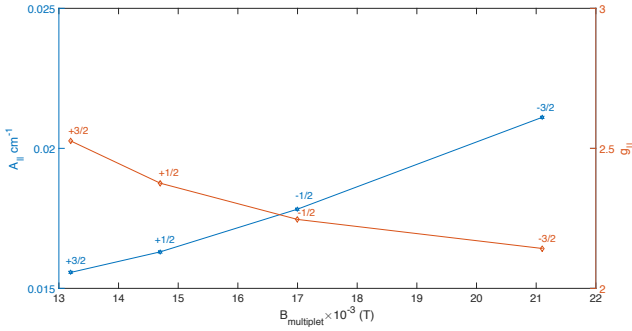


FIG. 5. g-factor anisotropy and hyperfine structure anisotropy of Cu^{2+} ion in nuclear perturbation.

oxygen 0.06 \AA from the Cu^{2+} ion. The increase of any copper-oxygen bond length of CuO_6 octahedral has a vital role in the formation of Jahn-Teller effect.

In the expressions for the hyperfine structure, the terms involving $\frac{\lambda}{\Delta}$ has been evaluated from the measurements of the g-factor anisotropies in the multi mode ESR spectrum mapping (Fig.2). Measured values of $A_{\parallel Cu}$ and calculated $A_{\perp Cu}$ can be regarded as determining two unknowns, $\langle r^{-3} \rangle$ and the core polarization parameter, k , using available values of $g_{\parallel Cu}^I$. To explain the hyperfine structure broadening, the second order correction term $\sim (\frac{\lambda}{\Delta})^2$ is useful for the case of a rhombic distortion which admixes the ground state $|x^2 - y^2\rangle = |2^s\rangle$ with $|3z^2 - r^2\rangle = |0\rangle$ and broaden the hyperfine structure about $79 G$.

An angle, ϕ , is corresponded to a lower symmetry, and the corresponding eigenstates are; ground state $\cos\frac{\phi}{2} |x^2 - y^2\rangle + \sin\frac{\phi}{2} |3z^2 - r^2\rangle$ with the orthogonal excited state $\sin\frac{\phi}{2} |x^2 - y^2\rangle - \cos\frac{\phi}{2} |3z^2 - r^2\rangle$ which is higher in energy by $4 \times (\text{Jahn - Teller energy } W_{JT})^{35,39,43}$. Hence, the admixture of the excited state is given by $\sin^2(\frac{\phi}{2})$ for this lower symmetry distortion⁴⁰. From this experiment results, it may be estimated as $\phi \sim \tan^{-1}(\frac{79}{132+147+170+211}) = 6.82^\circ$ (Fig.3), and which means that the admixture is about 0.36%. This estimation of angle is nearly equal to the calculated angle using the metal-ligand bond lengths of CuO_6 octahedral structure.

2. Jahn-Teller effect and parameters:

The observed broadening $79 G$ of the Cu^{2+} ion hyperfine structure or multiplet (Fig. 2, 3 and 4) along the increase of magnetic field may be explained by nuclear quadruple interaction in the symmetry of the ligand field of CuO_6 octahedral in the $SrLaAlO_4$ crystal. Nuclear displacement of copper lowers the symmetry of CuO_6 producing a special coupling between the electronic and nuclear motion³⁹.

In the distorted rhombic lower symmetry of CuO_6 structure at $20mK$ supports the occurrence of a static Jahn-Teller effect (*SJTE*). Burns and Hawthorne⁸ showed that the state of lowest energy in which octahedron suffers an elongation in tetragonal symmetry are corresponded to a *SJTE*. Hence with the elongation in the octahedron ligand complex CuO_6 under rhombic deformation in $SrLaAlO_4$ tetragonal crystal, the variation of measured hyperfine multiplet widths $-155.7 \times 10^{-4} \text{ cm}^{-1}$ (13.2 mT), $-163.0 \times 10^{-4} \text{ cm}^{-1}$ (14.7 mT), $-178.3 \times 10^{-4} \text{ cm}^{-1}$ (17.0 mT) and $-211.1 \times 10^{-4} \text{ cm}^{-1}$ (21.1 mT) with the order of nuclear magnetic quantum number $+\frac{3}{2}$, $+\frac{1}{2}$, $-\frac{1}{2}$, and $-\frac{3}{2}$ respectively at 9.072 GHz ($WG_{H_{4,1,1}}$) (Fig. 3) can be referred to the effect of *SJTE*.

Breen, Krupka and Williams⁹ found that the spin-lattice relaxation time (τ) at liquid helium temperature is about four orders of magnitude faster for Cu^{2+} in lanthanum magnesium nitrate than in tutton salt of tetragonal or lower symmetry of ligand field. They relate this result to the rate of relaxation ($\frac{1}{\tau}$) between equivalent distortions without reorientation of electron spin. Similarly, in continuous cooling, maximum Q-factor of WG modes were attained around $10K$ and decreased about ten times in magnitude at $20mK$ in $SrLaAlO_4$. It proves the increase of relaxation time at 20 mK .

Generally, a rhombic distortion is corresponded to principle g-factors in the direction of three mutually perpendicular four-fold axes of CuO_6 . These g-factors to the order $\frac{\lambda}{\Delta}$ are³⁵:

$$\begin{aligned} g_1 &= g_s - \frac{2\lambda}{\Delta} \{ \cos\frac{1}{2}\phi - \sqrt{3}\sin\frac{1}{2}\phi \}^2 \\ g_2 &= g_s - \frac{2\lambda}{\Delta} \{ \cos\frac{1}{2}\phi + \sqrt{3}\sin\frac{1}{2}\phi \}^2 \\ g_3 &= g_s - \frac{8\lambda}{\Delta} \{ \cos^2\frac{1}{2}\phi \}^2 \end{aligned} \quad (4)$$

Here, ϕ is the vectorial angle of a polar coordinate system (ρ, ϕ) which describes the $\Gamma_3(E)$ distortions corresponding to the normal-coordinates transformation $Q_\epsilon (= \rho \sin \phi)$ and $Q_\theta (= \rho \cos \phi)$. At the experiment

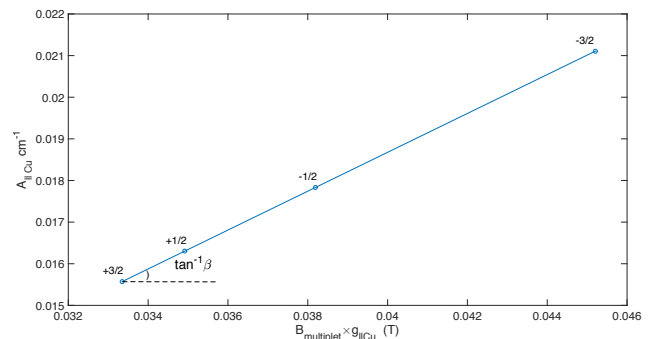


FIG. 6. Bohr magneton is revealed in hyperfine structure anisotropy of Cu^{2+} ion.

temperature 20 mK , g -factors along four-fold axes in the octahedral symmetry is corresponded to $g_3 > g_2 > g_1$ with the elongation along z -axis. In such a lower symmetry in the Jahn-Teller stabilization energy of the CuO_6 metal ligand system, an admixture of the ground state $|x^2 - y^2\rangle$ with the excited $|3z^2 - r^2\rangle$ state is evident under the condition $R = \frac{g_2 - g_1}{g_3 - g_2} < 1$ as implied for the elongation along z -axis⁴⁰. The observed hyperfine structure anisotropy follows the equation no.3 under condition $A_{\parallel Cu} \gg P_{\parallel}$. In the regular ESR spectrum of *Fig. 4*, the multiplet at $M_I = -\frac{3}{2}$ disappeared clearly due to local strain effect. Wei et al.³³ found that the $Cu - O1$ bond length increases shifting away the oxygen 0.06 \AA from the Cu^{2+} ion. From this significant amount of covalent bond length extension, it is plausible to say that the perturbation due to local strain is large in comparison with Zeeman anisotropy energy difference $(g_{\parallel Cu} - g_{\perp Cu})\beta B$.

The variation characteristics of $g_{\parallel Cu}$ and $A_{\parallel Cu}$ with respect to multiplet width in magnetic field, $B_{multiplet}$, has been shown in the *Fig. 5* with corresponding M_I . With the measured parameters $A_{\parallel Cu}$, $g_{\parallel Cu}$ and multiplet width in terms of magnetic field according to M_I , we found Bohr magneton $\beta = 9.23 \times 10^{-24} JT^{-1}$ from the graph in the *Fig. 6*. The characteristic straight line supports the theoretical predictions and consistency of this measurement. According to the equation no.3, the parameter, $P_{\parallel} = \frac{\Delta_a - \Delta_{-a}}{2} = 12.3 \times 10^{-4} cm^{-1}$, has been measured as an anisotropy of $A_{\parallel Cu}$ due to nuclear quadrupole moment (*Fig. 7*). This value of P_{\parallel} reveals $\langle r_q^{-3} \rangle = 5.23\text{ a.u.}$ with nuclear quadrupole moment $Q = -0.211\text{ barn}^{44}$. $\langle r^{-3} \rangle \simeq 7.5\text{ a.u.}$ for free cupric ion, and 6.3 a.u. is measured value of this ion in lanthanum magnesium nitrate⁴⁵. These values supports that $\langle r_q^{-3} \rangle = 5.23\text{ a.u.}$ in $SrLaAlO_4$ is valid.

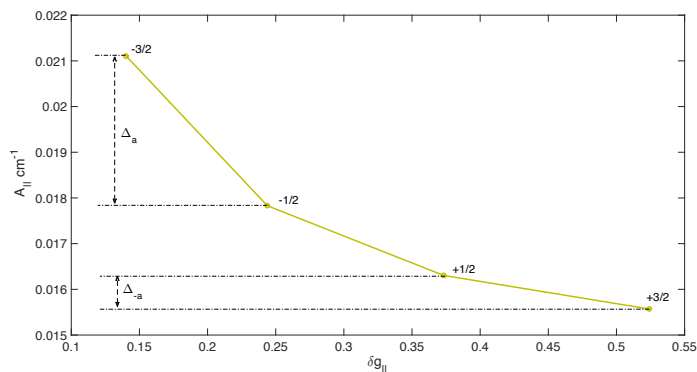


FIG. 7. Impacts of nuclear dipolar hyperfine structure parameter of Cu^{2+} ion in the substituted Al^{3+} ion site.

D. Conclusion:

High WG mode Q -factor in this crystal at $\leq 20\text{ mK}$ has allowed sensitive multi-mode ESR, and measurement of hyperfine structure anisotropy of spin along with site symmetry. The temperature was kept at $\leq 20\text{ mK}$ to observe the hyperfine multiplets. Rapid broadening of Cu^{2+} ion hyperfine structure due to static Jahn-Teller effect^{8,9,40} are underlined of nuclear quadruple moment in a lower symmetry of paramagnetic ion's site in the elongated CuO_6 octahedral structure^{39,46}. Ground state becomes unstable due to displacement of the copper nucleus in the centro-symmetric octahedron^{46,47}. At least two electronic states of the reference configuration should be involved in rationalization of structural changes in the polyatomic system. JTE is a transformation in the two electron state paradigm in formation, deformation, and transformation of molecular systems and solids^{48?, 49}. The hyperfine multiplet anisotropy measurement is valid only if $|\frac{P_{\parallel}}{A_{\parallel Cu}}|$ is quite small than unity. Determination of hyperfine line spacing and broadening as well as the justification of covalency contributes to the microscopic state analysis at millikelvin temperatures. This WG mode ESR spectroscopy shows an alternative process for the estimation of Bohr magneton and $\langle r_q^{-3} \rangle$. The results are noteworthy as the first example of nuclear quadruple interaction observation as an anisotropy of hyperfine structure using microwave WG multi mode ESR.

ACKNOWLEDGMENTS

This work was funded by Australian Research Council (ARC) Grant no.CE110001013. Thanks to Dr. Warwick G. Farr for assistance with data acquisition and Mr. Steve Osborne for technical support.

E. References:

- ¹G. Kurizki^{a,1}, P. Bertet^b, Y. Kubo^b, K. Mølmer^c, D. Petrosyan^{d,e}, P. Rabl^f, and J. Schmiedmayer^f, PNAS **112**, 3866 (2015).
- ²R. Dumke^{1,2,12}, Z. Lu³, J. Close⁴, N. Robins⁴, A. Weis⁵, M. Mukherjee^{2,6}, G. Birkl⁷, C. Hufnagel², L. Amico^{2,8,9}, M. G. Boshier¹⁰, K. Dieckmann², W. Li^{2,6}, and T. C. Killian¹¹, J.Opt. **18** (2016), 10.1088/2040-8978/18/9/093001.
- ³G. Binsky, R. Amsüss, J. Majer, D. Petrosyan, J. Schmiedmayer, and G. Kurizki, Quantum Inf Process **10**, 1037 (2011).
- ⁴I. Buluta¹, S. Ashhab^{1,2}, and F. Nori^{1,2}, Rep. Prog. Phys. **74** (2011) 104401 **74**, 104401 (2011).
- ⁵W. G. Farr, D. L. Creedon, M. Goryacheve, K. Benmessai, and M. E. Tobar, Phys. Rev. B **88**, 224426 (2013).
- ⁶K. Benmessai, W. G. Farr, D. L. Creedon, Y. Reshitnyk, J. M. Le-Floch, T. Duty, and M. E. Tobar, Phys. Rev. B **87**, 094412 (2013).
- ⁷M. E. Tobar, J. Krupka, E. N. Ivanov, and R. A. Woode, Journal of Physics D: Applied Physics **30**, 2770 (1997).
- ⁸P. C. Burns and F. C. Hawthorne, The Canadian Mineralogist **34**, 1089 (1996).

- ⁹D.P.Breen, D.C.Krupka, and F.I.B.Williams, *The Physical Review* **179**, 241 (1969).
- ¹⁰J. Goodenough, *Annu. Rev. Mater. Sci.* **28**, 1 (1998).
- ¹¹X. Li, X. Ma, D. Su, L. Liu, R. Chisnell, S. P. Ong, H. Chen, A. Toumar, J.-C. Idrobo, Y. Lei, J. Bai, F. Wang, J. W. Lynn, Y. S. Lee, and G. Ceder, *NATURE Materials* **13**, 586 (June 2014).
- ¹²M. Goryachev, W. G. Farr, and M. E. Tobar, *Appl. Phys. Lett.* **103**, 262404 (2013).
- ¹³W.-L. Feng and W.-C. Zheng, *Molecular Physics* **112**, 85 (2013).
- ¹⁴Wen-LinFeng^{a,b,c}, K. Wang^a, F. Zhao^a, and J.-Y. Xue^{a,c}, *Journal of Physics and Chemistry of Solids* **75**, 787 (2014).
- ¹⁵W.-L. Feng, *Materials Letters* **110**, 91 (2013).
- ¹⁶K. W. Xu Feng^a, Wenlin Feng^{a,b}, *Journal of Alloys and Compounds* **628**, 343 (2015).
- ¹⁷W.L.Feng^{a,c,e}, X. Li^a, W.C.Zheng^{b,e}, Y. Yang^b, and W. Yang^d, *Journal of Magnetism and Magnetic Materials* **323**, 528 (2011).
- ¹⁸J. Krupka, K. Derzakowski, M. E. Tobar, J. Hartnett, and R. G. Geyer, *Meas. Sci. Technol* **10**, 387 (1999).
- ¹⁹J.-M. L. Floch, Y. Fan, G. Humbert, Q. Shan, D. Férachou, R. Bara-Maillet, M. Aubourg, J. G. Hartnett, V. Madrangeas, D. Cros, J.-M. Blondy, J. Krupka, and M. E. Tobar, *Review of Scientific Instruments* **85**, 031301 (2014).
- ²⁰M. Gomilsek, Seminar: University of Ljubljana, Slovenia, Year:2012..
- ²¹J. Krupka and J. Mazierska, *IEEE Transactions On Microwave Theory And Techniques* **Special Issue**, 1 (2000).
- ²²J. G. Hartnett, M. E. Tobar, A. G. Mann, E. N. Ivanov, J. Krupka, and R. Geyer, *IEEE Transactions on Ultrasonics, Ferroelectrics, and Frequency Control* **46**, 993 (1999).
- ²³J. Charles P. Poole and H. A. Franch, *Handbook of Electron Spin Resonance*, Vol. 2 (Springer-Verlag, New York, 1999) Chap. Sensitivity, pp. 3–12.
- ²⁴G. Annino, M. Cassettari, I. Longo, and M. Martinelli, *Appl.Magn.Reson.* **16**, 45 (1999).
- ²⁵I. Longo, *Meas.Sci.Technol.* **2**, 1169 (1991).
- ²⁶A. Colligiani, *Appl. Magn. Reson.* **15**, 39 (1998).
- ²⁷J. Anders, A. Angerhofer, and G. Boero, *Journal of Magnetic Resonance* **86217**, 19 (2012).
- ²⁸Y. S. Yap, Y. Tabuchi, M. Negoro, and A. Kagawa, *Review of Scientific Instruments* **86**, 0631101 (2015).
- ²⁹A. G. Anna Pajaczkowska, *Prog. Crystal Growth and Charact.* **36**, 123 (1998).
- ³⁰A. Gloubokov, R. Jablonski, W. Ryba-Romanowski, j. Sassa, A. Pajaczkowska, R. Uecker, and Reiche, *Journal of Crystal Growth* **147**, 123 (1995).
- ³¹A. G. C. F. Woensdregt, H. W. M. Janssen and A. Pa-jaczkowska, *Journal of Crystal Growth* **171**, 392 (1997).
- ³²P. Aleshkevych, M. Berkowski, W. Ryba-Romanowski, and H. Szymczak, *Phys. Stat. sol. (b)* **218**, 521 (2000).
- ³³W.-H. Weia, S.-Y. Wua, and H.-N. Dong, *Z. Naturforsch* **60a**, 541 (March 2005).
- ³⁴J. R. Pilbrow, *Transition Ion Electron Paramagnetic Resonance* (Oxford University Press, Walton Street, Oxford OX2, UK, 1990) Chap. 1, pp. 3–61.
- ³⁵A. Abragam and B. Bleaney, *Electron Paramagnetic Resonance of Transition Ions* (Oxford University Press, 1970) Chap. Ions of the 3d group, pp. 365–490.
- ³⁶B. Bleaney, K. Bowers, and D. Ingram, *Proc. R. Soc. Lond.* **228**, 147 (1955).
- ³⁷B. Bleaney, K. Bowers, and R. Trenam, *Proc. R. Soc. Lond.* **228**, 157 (1955).
- ³⁸M. A. Hosain, J. -M. Le Floch, J. Krupka, and M. E. Tobar, *J. Magn. Reson.* **281**, 209 (2017).
- ³⁹I. B. Bersuker, *Che. Rev.* **101**, 1067 (2001).
- ⁴⁰S. K. Misra and C. Wang, *J. Phys.: Condens. Matter* **1**, 771 (1989).
- ⁴¹Y. V. Yablokov and T. Ivanova, *Coordination Chemistry Reviews* **190-192**, 1255 (1999).
- ⁴²Y. V. Yablokov, T. A. Ivanova, and A. E. Usachev, *JETP Lett.* **60**, 785 (Dec. 1994).
- ⁴³U. Opic and M. H. L. Pryce, *Proceedings of the Royal Society A* **238A**, 425 (1957).
- ⁴⁴N. Stone, *Atomic Data and Nuclear Data Tables* **90**, 75 (2005).
- ⁴⁵B. Bleaney, K. Bowers, and H. Pryce, *Proc. R. Soc. Lond.* **228**, 166 (1955).
- ⁴⁶I. B. Bersuker, *Journal of Physics* **428**, 012028 (2013).
- ⁴⁷I. B. Bersuker, *Appl. Phys. Lett.* **107**, 202904 (2015).
- ⁴⁸V. Polinger, P. Garcia-Fernandez, and I. B. Bersuker, *Physica B* **457**, 296 (2015).
- ⁴⁹I. B. Bersuker, *Applied Physics Letters* **106**, 022903 (2015).